axioms

MDPI

Article

Detachment Waves in Frictional Contact II: Analysis and Simulations of a Three-Mass System

Jeongho Ahn [1,*] and Meir Shillor [2]

[1] Department of Mathematics and Statistics, Arkansas State University, Jonesboro, AR 72464, USA
[2] Department of Mathematics and Statistics, Oakland University, 146 Library Drive, Rochester, MI 48309, USA; shillor@oakland.edu
* Correspondence: jahn@astate.edu

Abstract: This work continues the study of a mathematical model for the motion of a mass–spring–damper system with friction. There, a two-mass model was constructed, its solvability established, the steady states investigated, and numerical simulations presented. The main interest here is in the modeling, analysis of the steady states, and simulation of a three-mass system—in particular, in the propagation of detachment or slip waves, which happen when the system transits from a stick state to a slip motion. The introduction of friction changes the problem into systems of three differential set-valued inclusions, which are mathematically and computationally very challenging. The analysis of the steady states shows the regions of stick, where there is enough frictional resistance that prevents motion. The proposed numerical methods are implemented, and the simulations show some representative types of system behavior, especially the cases of detachment waves. Some of the numerical simulations specifically support the theoretical analysis of slip initiation, reachability, and energy balance.

Keywords: detachment waves; differential set-valued inclusion; friction; stick states; sliding initiation; energy balance; numerical schemes

MSC: 74M10; 34A60; 49J53; 34C15; 34C26



Academic Editor: Giovanni Nastasi

Received: 21 March 2025
Revised: 8 April 2025
Accepted: 9 April 2025
Published: 15 April 2025

Citation: Ahn, J.; Shillor, M. Detachment Waves in Frictional Contact II: Analysis and Simulations of a Three-Mass System. *Axioms* **2025**, *14*, 299. https://doi.org/10.3390/axioms14040299

Copyright: © 2025 by the authors. Licensee MDPI, Basel, Switzerland. This article is an open access article distributed under the terms and conditions of the Creative Commons Attribution (CC BY) license (https://creativecommons.org/licenses/by/4.0/).

1. Introduction

This work deals with the stick–slip states of a 'simple' system with friction and is a continuation of [1,2]. It has two main objectives, the first of which is to continue our mathematical and numerical study of the initiation of motion in a system of masses that we started in [1,2] and, eventually, to study the detachment or slip waves in continuous systems. To that end, we consider a system of three masses connected with springs and dampers that are on a straight rail and may move under the action of an applied force, while friction resists the motion. The system is 'simple'; however, mathematically, it is formulated as a system of ordinary differential inclusions, which is of interest in and of itself. The second objective is to make the system amenable to simpler analysis, bypassing many of the technical details related to higher dimensions and weak convergence. Therefore, it is another contribution to the currently maturing Mathematical Theory of Contact Mechanics (MTCM), as it also provides an example of the application of very abstract theorems established in [3].

The importance of such slip waves is hard to overstate, as they take place in many engineering and physical settings, such as car brakes, walking on a slippery surface, crumbling of concrete structures, motion of tectonic plates, and a host of others. Moreover,

there exists literature about the application of such waves in geology (see, e.g., [4,5] and the references therein).

This mathematical study of detachment or sliding waves in systems with friction is motivated by the important experimental works [6,7] where the sliding or detachment waves were experimentally visualized. In our case, the mass–spring–damper system with three masses is, essentially, an initial setting where we can simulate the beginning of a sliding wave. It is simple enough to deal with conceptually and numerically but allows the study of the onset of sliding in a system with friction. Indeed, when the force applied to the first mass is increased beyond the *friction bound*, the mass will start sliding and will continue moving as long as the total force acting on it is above the bound. Then, when the force is sufficient to overcome the frictional resistance of the third mass, the whole system will slide; this movement will constitute a detachment wave. This work is just a step in the study, and we make some comments, observations, and remarks. The work will be continued by using numerical simulations and extended as indicated in the conclusions section, where we also describe some ideas for future work.

A related body of work, mostly computer modeling and simulations, can be found in [8,9], where the Cattaneo theory of frictional contact is extended to elastic half-spaces in contact through rough disordered interfaces.

To simulate the solutions, we use the so-called one-step θ schemes (see, e.g., [10] and the references therein), together with finite difference methods (FDMs). In addition, a regularization technique is used to apply the Newton–Raphson method effectively, since friction introduces non-smoothness into the problem. The simulations are found to be fast and efficient and show typical baseline behavior as well as the development of sliding or detachment waves. We also present a comparison of the computations with different θ values. We note that $\theta = 1/2$ and $\theta = 1$ are the Crank–Nicolson and Implicit Euler schemes, respectively. We establish the energy balance in the system, and it is found that our schemes preserve it. Moreover, we deal with the topic of reachability, that is, which steady states can be obtained as limits of dynamical evolution. It seems, numerically, that each one can be reached as a limit of the process with properly chosen initial conditions.

MTCM is currently reaching a mature state, and there are many recent monographs dedicated to various aspects of the theory. We mention only a few dealing with modeling and theory [11–13] and those that address the computational and numerical aspects [14–16]. The topics and results deal with the many different aspects of MTCM systems, which include the processes of contact, friction, bonding and debonding, and surface wear or damage. The present work is a contribution to this growing body of knowledge.

Following this introduction, Section 2 constructs in detail a set of three-mass models, Models 1–3, for the dynamic, quasistatic, and static cases. The first describes the dynamic motion of a three-mass spring–damper system with friction. The quasistatic model is obtained when the accelerations in the system are neglected. The third one describes the steady states, or *stick states*, and the introduction of friction leads to a continuum of steady states. Even though the models are 'simple', the addition of friction turns them into differential set-valued inclusions, with the related mathematical complexity. Section 3 contains an analysis of Problem 3 and describes the system's steady states. As is almost always the case when friction is present, it is found that the system has a continuum (or two) of steady states.

The problem is constructed in a very abstract setting in Section 4. The existence and uniqueness of the weak solution of the dynamic problem, Problem 1, and the existence of a solution of the quasistatic problem, Problem 2, are proved in Section 4, using the very general existence and uniqueness theorem for differential pseudomonotone operators as established in [3]. Section 5 is short and begins the study of the initiation of slip, as well as

the approach to steady stick states. Section 6 investigates a form of energy balance in the mass system.

Section 7 presents detailed numerical schemes. Section 8 shows the results of the baseline simulation and the case of a slip wave. Section 9 describes three issues related to the numerical scheme. In Section 9.1, we assess and graphically display the performance of the three schemes. Section 9.2 briefly discusses the question of reachability of steady states from initial conditions. In Section 9.3, we prove and numerically display that our numerical scheme conserves energy.

Section 10 presents a few conclusions, unresolved issues, and some future directions; indeed, we believe that this research into stick–slip waves is of considerable interest, both practical and theoretical, and we plan to continue it in the near future.

2. The Model

We model a 'simple' setting of three masses connected with springs and dampers that vibrate, in the presence of friction. This leads to the related dynamic, quasistatic, and static set-valued problems.

The mass–spring–damper system consists of three coupled masses that can move, as a result of an applied force f, on a straight horizontal rail, where frictional resistance to the motion is taken into account. We follow the construction in [1], and the setting is depicted in Figure 1.

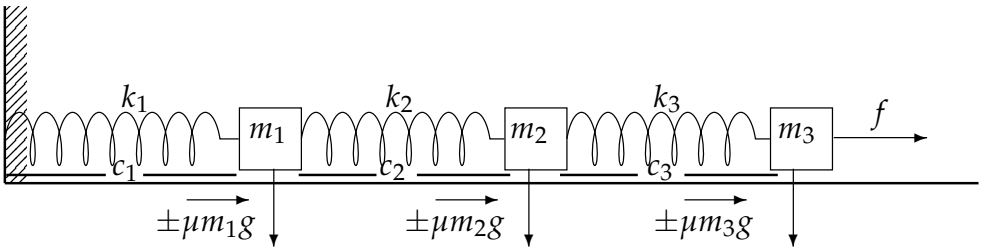


Figure 1. The masses are m_i, the spring constants are k_i, and the damping coefficients are c_i for $i = 1, 2, 3$. Frictional resistance $\mu m_i g$ opposes the motion of each mass.

We let $i = 1, 2, 3$ everywhere below, and we denote as $x_i = x_i(t)$ the displacement of the mass i at time t from an equilibrium position $\hat{x}_i$ in which the three springs are neither stretched nor compressed. The damping coefficients are c_i, while k_i denote the spring constants. We denote as μ the friction coefficient, which is assumed to depend on the speed and is the same for all three masses; we use g to denote the gravitational acceleration. The prime denotes the time derivative, and the velocities are $v_i = x_i'$. A force f is applied to the mass m_3, while the left end of spring k_1 is attached to a fixed support. The maximal frictional resistance to the motion of each mass is $\mu m_i g$ and is opposite to the motion. When body m_i moves to the right, $v_i > 0$, the friction force is $-\mu m_i g$, and when it moves to the left, the friction force is $\mu m_i g$. When the body is stationary, $v_i = x_i' = 0$, the frictional resistance *exactly* balances the forces that act on the mass m_i. Using the usual arguments, the inertial terms and forces balance yield the following system of equations:

$$\begin{cases} m_1 x_1'' = p_1 \equiv -c_1 v_1 + c_2(v_2 - v_1) - k_1(x_1 - \hat{x}_1) + k_2((x_2 - \hat{x}_2) - (x_1 - \hat{x}_1)) \\ \qquad\qquad -\text{sig}(v_1)\mu m_1 g, \\ m_2 x_2'' = p_2 \equiv -c_2(v_2 - v_1) + c_3(v_3 - v_2) - k_2((x_2 - \hat{x}_2) - (x_1 - \hat{x}_1)) \\ \qquad\qquad +k_3((x_3 - \hat{x}_3) - (x_2 - \hat{x}_2)) - \text{sig}(v_2)\mu m_2 g, \\ m_3 x_3'' = p_3 \equiv f - c_3(v_3 - v_2) - k_3((x_3 - \hat{x}_3) - (x_2 - \hat{x}_2)) \\ \qquad\qquad -\text{sig}(v_3)\mu m_3 g, \\ |p_i| \le \mu m_i g \implies v_i = 0, \qquad i = 1, 2, 3. \end{cases} \tag{1}$$

Here, $\text{sig}(v) = 1$ when $v > 0$, and $\text{sig}(v) = -1$ when $v < 0$. However, the use of the $\text{sig}(v)$ function is insufficient to describe the frictional stick regions (when $v = 0$), therefore, we replace it with the *subdifferential* of $|v|$, which is the set-valued function,

$$\partial|v| = \begin{cases} 1 & v > 0, \\ [-1, 1] & v = 0, \\ -1 & v < 0. \end{cases}$$

The interval $[-1, 1]$, when $v = 0$, captures the *stick region*, where friction exactly blocks any motion.

For notational simplicity, we set

$$\overline{x}_1 = x_1 - \hat{x}_1, \quad \overline{x}_2 = x_2 - \hat{x}_2, \quad \overline{x}_3 = x_3 - \hat{x}_3,$$

and we omit the overbar in the following. Thus, x_i is the displacement of mass m_i from the steady position in which the springs are at their natural lengths.

We may now write (1) in a concise form as a system of *differential inclusions*. Specifically, the dynamic model for the motion with damping and friction of a system of three coupled masses is as follows:

Problem 1 (Dynamic)**.** *Given positive constants m_i, k_i, c_i, g, for $i = 1, 2, 3$ and the functions $f = f(t)$ and $\mu = \mu(v)$, find $(x_1, v_1, x_2, v_2, x_3, v_3) : [0, T] \to \mathbb{R}^6$ such that*

$$v_i = x_i', \tag{2}$$

$$m_1 v_1' + c_1 v_1 - c_2(v_2 - v_1) + k_1 x_1 - k_2(x_2 - x_1) \in -\partial|v_1|\mu m_1 g, \tag{3}$$

$$m_2 v_2' + c_2(v_2 - v_1) - c_3(v_3 - v_2) + k_2(x_2 - x_1) - k_3(x_3 - x_2) \in -\partial|v_2|\mu m_2 g, \tag{4}$$

$$m_3 v_3' + c_3(v_3 - v_2) + k_3(x_3 - x_2) \in f - \partial|v_3|\mu m_3 g, \tag{5}$$

together with the initial conditions $x_i(0) = \overline{x}_i, v_i(0) = \overline{v}_i$.

We note that the actual initial positions are $\overline{x}_i + \hat{x}_i$. For simplicity, we use the same coefficient of friction function $\mu = \mu(v)$ for the three masses, which means that the surface and the masses have the same friction characteristics. It is straightforward to use three different friction coefficients when the friction characteristics are different. It is assumed that μ is a bounded, positive, and continuous function of v. The case where μ is discontinuous, actually set-valued, at $\{v = 0\}$ was studied in [17].

In the following section, we express the problem in an abstract form and show that it has a unique weak solution.

The *quasistatic* version of the problem is obtained by neglecting the accelerations in the system, which is a valid approximation when the force f changes slowly with time and the initial conditions are close to equilibrium. Therefore, the *quasistatic* version of the problem is as follows:

Problem 2 (Quasistatic)**.** *Given positive constants m_i, k_i, c_i, g, for $i = 1, 2, 3$ and the functions $f = f(t)$ and $\mu = \mu(v)$, find $(x_1, v_1, x_2, v_2, x_3, v_3) : [0, T] \to \mathbb{R}^6$ such that*

$$v_i = x_i', \tag{6}$$
$$c_1 v_1 - c_2(v_2 - v_1) + k_1 x_1 - k_2(x_2 - x_1) \in -\partial|v_1|\mu m_1 g, \tag{7}$$
$$c_2(v_2 - v_1) - c_3(v_3 - v_2) + k_2(x_2 - x_1) - k_3(x_3 - x_2) \in -\partial|v_2|\mu m_2 g, \tag{8}$$
$$c_3(v_3 - v_2) + k_3(x_3 - x_2) \in f - \partial|v_3|\mu m_3 g, \tag{9}$$
$$x_i(0) = \overline{x}_i. \tag{10}$$

Note that in this case, the initial conditions are only for displacements. We show the existence of a solution to this problem in Section 4; however, the uniqueness of the solutions remains open.

Finally, the *static* problem, when the system is motionless, with a constant applied force f, is as follows:

Problem 3 (Static)**.** *Given positive constants m_i, k_i, g, for $i = 1, 2, 3$ along with a constant f and $\mu = \mu(0)$, find the displacements $(x_1, x_2, x_3) \in \mathbb{R}^3$ such that*

$$k_1 x_1 + k_2(x_1 - x_2) \in -\partial|0|\mu(0) m_1 g, \tag{11}$$
$$k_2(x_2 - x_1) + k_3(x_2 - x_3) \in -\partial|0|\mu(0) m_2 g, \tag{12}$$
$$k_3(x_3 - x_2) \in f - \partial|0|\mu m_3 g. \tag{13}$$

Note that in this case, there are no initial conditions. We study the problem in the next section and show, as expected, that it has a continuum of solutions.

We note that the assumption that $f = const.$ in the static case can be relaxed, and the results hold true in the case of a time-dependent $f = f(t)$, as long as the resultant force acting on mass m_3 remains below the friction bound $\mu m_3 g$. This is another peculiarity of friction.

The problems are clearly related; however, each has a different mathematical structure. The analysis of the problems is presented in the following sections. Whereas the time-dependent problems are 'simple' to state, casting them in variational form allows one to use them as examples of the general existence theory in MTCM.

3. Steady (Stick) States—Analysis of Problem 3

We begin the analysis with the system's steady states. It is found, as expected when friction is present, that there is a continuum of such states. Indeed, let $(x_1, x_2, x_3) \in \mathbb{R}^3$ be the solutions of the static problem. Then, it follows from (11)–(13) that

$$\begin{aligned} |k_1 x_1 + k_2(x_1 - x_2)| &\leq \mu m_1 g, \\ |k_2(x_2 - x_1) + k_3(x_2 - x_3)| &\leq \mu m_2 g, \\ |k_3(x_3 - x_2) - f| &\leq \mu m_3 g. \end{aligned} \tag{14}$$

Here and below, for simplicity, we write μ instead of $\mu(0)$, since $v_i = 0$. Hence, for a given force $f \geq 0$, we find

$$-\mu m_1 g \le (k_1+k_2)x_1 - k_2 x_2 \le \mu m_1 g,$$
$$-\mu m_2 g \le -k_2 x_1 + (k_2+k_3)x_2 - k_3 x_3 \le \mu m_2 g,$$
$$f - \mu m_3 g \le -k_3 x_2 + k_3 x_3 \le f + \mu m_3 g.$$

It follows that

$$-\frac{\mu m_1 g}{k_1+k_2} + \frac{k_2}{k_1+k_2}x_2 \le x_1 \le \frac{\mu m_1 g}{k_1+k_2} + \frac{k_2}{k_1+k_2}x_2.$$

Then, through straightforward algebraic manipulations of the second inequality using the first, we obtain

$$-ab\mu g + \frac{ak_3}{k_2+k_3}x_3 \le x_2 \le ab\mu g + \frac{ak_3}{k_2+k_3}x_3,$$

where we set

$$a = \frac{(k_1+k_2)(k_2+k_3)}{k_1k_2+k_2k_3+k_1k_3}, \qquad b = \frac{m_2}{k_2+k_3} + \frac{m_1k_2}{(k_1+k_2)(k_2+k_3)}.$$

The third inequality leads to

$$\frac{d}{k_3}f - \left(\frac{dm_3}{k_3} + abd\right)\mu g \le x_3 \le \frac{d}{k_3}f + \left(\frac{dm_3}{k_3} + abd\right)\mu g,$$

where

$$d = \frac{k_1k_2+k_2k_3+k_1k_3}{k_1k_2}.$$

Next, let

$$L_3^- = \frac{d}{k_3}f - l_3, \quad L_3^+ = \frac{d}{k_3}f + l_3, \quad l_3 = \left(\frac{dm_3}{k_3} + abd\right)\mu g. \tag{15}$$

$$L_2^- = -ab\mu g + \frac{ak_3}{k_2+k_3}L_3^-, \qquad L_2^+ = ab\mu g + \frac{ak_3}{k_2+k_3}L_3^+. \tag{16}$$

$$L_1^- = -\frac{m_1\mu g}{k_1+k_2} + \frac{k_2}{k_1+k_2}L_2^-, \qquad L_1^+ = \frac{m_1\mu g}{k_1+k_2} + \frac{k_2}{k_1+k_2}L_2^+. \tag{17}$$

The *stick regions*, where the three masses are stationary, are the intervals about the centers $\hat{x}_i$, for $i = 1, 2, 3$, given by

$$L_i^- \le x_i \le L_i^+. \tag{18}$$

Similar manipulations lead to the expressions obtained when $f < 0$; it should be noted that, because of the initial conditions and the structure of the problem, it is not symmetric with respect to f.

We conclude that, with the introduction of friction, the system has a whole range or continuum of steady states, which are the *stick states*. We recall (18) and that the actual positions of the masses are $x_i - \hat{x}_i$. We summarize our results as follows.

Proposition 1. *Assume that $f \ge 0$; then, the stick states or steady states of the system are*

$$L_i^- \le x_i - \hat{x}_i \le L_i^+, \tag{19}$$

where L_i^+, L_i^- are given in (15)–(17).

We note that depending on the system coefficients, it may happen that $L_1^+ \geq L_2^-$, in which case all the steady solutions of m_1 and m_2 occupy the interval $[L_1^-, L_2^+]$, and similar observations hold for the other possibilities. See Figure 2 below.

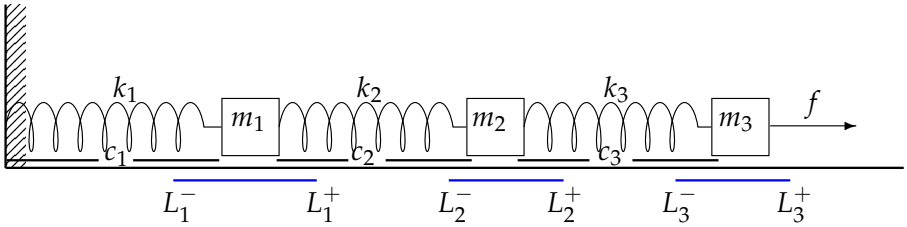


Figure 2. The possible steady states (blue) of each mass, according to (19).

Next, we briefly discuss the stability and reachability of the steady states. When the system is slightly perturbed, while it is inside the stationary interval, so that the inequalities in (19) are strict, the system remains stationary; hence, the state is stable but is not attracting (asymptotically stable). In the case of an equality, such as $x_1 - \hat{x}_1 = L_1^+$, the state is stable from the left and both stable and attracting from the right. Indeed, when the system perturbation is to the left of L_1^+, the system will stay there, and so it is stable. When the perturbation is to the right of L_1^+, the system will move toward L_1^+; hence, it is stable and attracting. The other possible cases behave similarly. It is seen that systems with friction exhibit behaviors that are outside of the standard stability theory.

Concerning *reachability*, we note that each steady state can be attained when the masses are positioned at the prescribed locations with zero initial velocities. The more interesting reachability question is which steady states can be reached as long-time limits of the dynamic or quasistatic solutions. Indeed, given $f = const.$ and $\widetilde{x}_i \in [\hat{x}_i - L_i^-, \hat{x}_i + L_i^+]$, can we find initial conditions $(\overline{x}_i, \overline{v}_i)$ that are *not* steady states such that the solutions of Problem 1 or Problem 2, starting at $(\overline{x}_i, \overline{v}_i)$ in the dynamic case and at $\overline{x}_i$ in the quasistatic case, converge, i.e., $(x_i(t), v_i(t)) \to (\widetilde{x}_i, 0)$ as $t \to \infty$? It seems that at this stage of our research, numerical experiments are the best way to gain insight into this reachability question. Our conjecture is that for each steady state, one can indeed find such initial conditions, and in the quasistatic case, these may not be unique.

4. Abstract Formulation of Problems 1 and 2

We study the two time-dependent problems, namely, Problems 1 and 2. It turns out that both the dynamic and quasistatic problems can be cast as degenerate evolution equations; however, the existence of their solutions is established by different versions of an abstract theorem.

The system is written as a first-order system in (2)–(5) and (6)–(10) in a unified way, as follows:

$$\begin{aligned}
&v_i = x_i', \\
&\alpha m_1 v_1' + c_1 v_1 - c_2(v_2 - v_1) + k_1 x_1 - k_2(x_2 - x_1) \in -\partial|v_1|\mu m_1 g, \\
&\alpha m_2 v_2' + c_2(v_1 - v_2) - c_3(v_3 - v_2) + k_2(x_2 - x_1) - k_3(x_3 - x_2) \in -\partial|v_2|\mu m_2 g, \\
&\alpha m_3 v_3' + c_3(v_3 - v_2) + k_3(x_3 - x_2) \in f - \partial|v_3|\mu m_3 g,
\end{aligned} \tag{20}$$

where, in the dynamic problem, $\alpha = 1$ and the initial conditions are $x_i(0) = \overline{x}_i$, $v_i(0) = \overline{v}_i$, and in the quasistatic problem, $\alpha = 0$ and the initial condition is $x_i(0) = \overline{x}_i$ for $i = 1, 2, 3$.

We will now proceed to reformulate the problem in an abstract setting as a variational formulation. Let $V = \mathbb{R}^6 = V^{'}$, where the prime denotes the dual space. We define a set-valued operator $A : L^2(0,T;V) \to L^2(0,T;V)$ to be

$$A\begin{pmatrix} x_1 \\ v_1 \\ x_2 \\ v_2 \\ x_3 \\ v_3 \end{pmatrix} = \begin{pmatrix} -v_1 \\ c_1v_1 - c_2(v_2 - v_1) + k_1x_1 - k_2(x_2 - x_1) \\ -v_2 \\ c_2(v_2 - v_1) - c_3(v_3 - v_2) + k_2(x_2 - x_1) - k_3(x_3 - x_2) \\ -v_3 \\ c_3(v_3 - v_2) + k_3(x_3 - x_2) \end{pmatrix} + g\begin{pmatrix} 0 \\ \mu(v_1)m_1\partial|v_1| \\ 0 \\ \mu(v_2)m_2\partial|v_2| \\ 0 \\ \mu(v_1)m_1\partial|v_3| \end{pmatrix}. \tag{21}$$

To simplify the notation, we define $\widetilde{A}$ as

$$\widetilde{A}z = \begin{pmatrix} 0 & -1 & 0 & 0 & 0 & 0 \\ k_1 + k_2 & c_1 + c_2 & -k_2 & -c_2 & 0 & 0 \\ 0 & 0 & 0 & -1 & 0 & 0 \\ -k_2 & -c_2 & k_2 + k_3 & c_2 + c_3 & -k_3 & -c_3 \\ 0 & 0 & 0 & 0 & 0 & -1 \\ 0 & 0 & -k_3 & -c_3 & k_3 & c_3 \end{pmatrix}\begin{pmatrix} x_1 \\ v_1 \\ x_2 \\ v_2 \\ x_3 \\ v_3 \end{pmatrix}.$$

Next, for a given z, we let $\zeta = (\xi_1, \eta_1, \xi_2, \eta_2, \xi_3, \eta_3)^T$ be a vector such that

$$\zeta \in g\begin{pmatrix} 0 \\ \mu(v_1)m_1\partial|v_1| \\ 0 \\ \mu(v_2)m_2\partial|v_2| \\ 0 \\ \mu(v_3)m_3\partial|v_3| \end{pmatrix}. \tag{22}$$

Then, we may write $Az = \widetilde{A}z + \zeta$, where ζ is the set-valued part of A. We also define a linear operator B as

$$B = \begin{pmatrix} 1 & 0 & 0 & 0 & 0 & 0 \\ 0 & \alpha & 0 & 0 & 0 & 0 \\ 0 & 0 & 1 & 0 & 0 & 0 \\ 0 & 0 & 0 & \alpha & 0 & 0 \\ 0 & 0 & 0 & 0 & 1 & 0 \\ 0 & 0 & 0 & 0 & 0 & \alpha \end{pmatrix}\begin{pmatrix} x_1 \\ v_1 \\ x_2 \\ v_2 \\ x_3 \\ v_3 \end{pmatrix}. \tag{23}$$

The unified abstract form of Problems 1 and 2 is as follows:

Problem 4. *Let $f \in C([0,T];\mathbb{R})$. Find $\boldsymbol{z} \in L^2(0,T;V)$ such that*

$$B\frac{d\boldsymbol{z}}{dt} + A\boldsymbol{z} \ni \boldsymbol{f}, \tag{24}$$

$$\boldsymbol{z}(0) = (x_{10}, \alpha v_{10}, x_{20}, \alpha v_{20}, x_{30}, \alpha v_{30})^T, \tag{25}$$

where $\boldsymbol{f} = (0, k_2(\hat{x}_1 - \hat{x}_2), 0, k_2(\hat{x}_2 - \hat{x}_1) + k_3(\hat{x}_2 - \hat{x}_3), 0, f + k_3(\hat{x}_3 - \hat{x}_2))^T$.

Here, the time derivative is understood in the sense of distributions. In the dynamic problem, $\alpha = 1$, and in the quasistatic one, $\alpha = 0$; we note that the quasistatic problem is degenerate. The existence and uniqueness results concerning Problem 4 are presented in the following theorem:

Theorem 1. *Assume that $\boldsymbol{f} \in C([0,T];V)$; then, systems (24) and (25) have a unique solution for $\alpha = 1$ and has a solution for $\alpha = 0$.*

The proof of Theorem 1 is very similar to the one presented in [1], since the abstract version is essentially the same problem. The proof there is based on the basic existence theorem in [3] for set-valued pseudomonotone operators. In the existence theorem, we need to show that the operator A is bounded, weakly coercive, and pseudomonotone, since the operator B is constant. In our 'simple' setting, the first two properties are straightforward to show, while the pseudomonotonicity holds in the dynamic case but not in the quasistatic case.

We note that Theorem 1 guarantees the existence of the so-called *weak solution*, i.e., the solution is only in $L^2(0,T;V)$. However, on every time interval $[t_a, t_b]$, where $v_1(t) \neq 0, v_2(t) \neq 0, v_3(t) \neq 0$, the solution is classical, since the subdifferentials are just functions on such intervals. Similarly, the solution is classical on every interval $[t_c, t_d]$, where $v_1(t) = v_2(t) = v_3(t) = 0$. Other types of intervals where the solution is classical are also possible.

As noted in [1], it may be of interest to clarify whether the lack of uniqueness in the quasistatic problem is related to the existence of a continuum of steady solutions.

5. Slip Initiation

We now provide a few observations on the initiation of slip in Problems 1 and 2. We assume, for the sake of simplicity, that $\mu = const. > 0$ and let the force f vary in time. First, we assume that f changes slowly, such that we are in the setting of the quasistatic problem. Later, we will relax this condition.

Let $f > 0$ and L_i^+ be given by (15)–(17), for the value of $f(0)$, and assume that the initial positions are at the right ends of the steady-state intervals, $x_{i0} = \hat{x}_i + L_i^+$, and $v_{i0} = 0$. Then, any increase in the force f will move the system away from the steady state, and so it will initiate sliding of all the masses, i.e., slip motion of the system.

On the other hand, if initially $x_{i0} = \hat{x}_i$, and $v_{i0} = 0$, and the force is increased above μm_3, the first mass m_3 starts sliding, extending spring k_3, while the the other two masses stay stationary, since there is sufficient frictional resistance to prevent their motion. As f is further increased, at some value when it exceeds $\mu(m_2 + m_3) + k_3(L_3^+ - L_2^+)$, mass m_2 also starts sliding. Then, when f is further increased, crossing the value $f^* = \mu(m_1 + m_2 + m_3) + k_3(L_3^+ - L_2^+) + k_2(L_2^+ - L_1^+)$ mass m_1 will start sliding, and the *detachment wave* arrives at m_1, so that all the masses are in motion.

6. Energy Balance

Since damping and frictional dissipation cause energy decay, the system eventually reaches a steady state, in which the force is constant. We deduce the system's energy

balance and let $c_1 = c_2 = c_3 = 0$, since we are interested in the frictional dissipation. We multiply Equation (2) with $x_1' = v_1$, Equation (3) with $x_2' = v_2$, and Equation (4) with $x_3' = v_3$, and we integrate over time. We note that $\partial|v_i|v_i = |v_i|$ and use (24) and (25) to find

$$\begin{aligned}
&\frac{\alpha}{2}\Big(m_1\Big(v_1^2(t) - v_{10}^2\Big) + m_2\Big(v_2^2(t) - v_{20}^2\Big) + m_3\Big(v_3^2(t) - v_{30}^2\Big)\Big)\\
&\quad + \frac{1}{2}(k_1 + k_2)\Big(x_1^2(t) - x_{10}^2\Big) + \frac{1}{2}(k_2 + k_3)\Big(x_2^2(t) - x_{20}^2\Big)\\
&\quad + \frac{1}{2}k_3\Big(x_3^2(t) - x_{30}^2\Big) = \int_0^t k_2(x_2v_1 + x_1v_2) + k_3(x_3v_2 + x_2v_3)d\tau\\
&\quad - m_1g\int_0^t \mu(v_1)|v_1|d\tau - m_2g\int_0^t \mu(v_2)|v_1|d\tau\\
&\quad - m_3g\int_0^t \mu(v_3)|v_3|d\tau + \int_0^t fv_3d\tau.
\end{aligned}$$

Here, we use the facts that, when $\alpha = 1$ (the dynamic case),

$$\int_0^t \frac{1}{2}(v_i^2)'ds = \frac{1}{2}(v_i^2(t) - v_{i0}^2), \quad \int_0^t \frac{1}{2}(x_i^2)'ds = \frac{1}{2}(x_i^2(t) - x_{i0}^2),$$

which represents the changes in the kinetic and elastic energy of masses $i = 1, 2, 3$. We let the total system energy at time t be

$$E(t) = E_k(t) + E_p(t),$$

where

$$\begin{aligned}
E_k(t) &= \frac{\alpha}{2}\Big(m_1v_1^2(t) + m_2v_2^2(t) + m_3v_3^2(t)\Big) \text{ and}\\
E_p(t) &= \frac{1}{2}\Big((k_1 + k_2)x_1^2(t) + (k_2 + k_3)x_2^2(t) + k_3x_3^2(t)\Big).
\end{aligned}$$

The *energy balance* in this system is

$$\begin{aligned}
E(t) = \; & E(0) + \int_0^t k_2(x_2v_1 + x_1v_2) + k_3(x_3v_2 + x_2v_3)d\tau\\
& - m_1g\int_0^t \mu(v_1)|v_1|d\tau - m_2g\int_0^t \mu(v_2)|v_1|d\tau\\
& - m_3g\int_0^t \mu(v_3)|v_3|d\tau + \int_0^t fv_3d\tau,
\end{aligned} \tag{26}$$

where

$$\begin{aligned}
E(0) &= E_k(0) + E_p(0)\\
&= \frac{\alpha}{2}\Big(m_1v_{10}^2 + m_2v_{20}^2 + m_3v_{30}^2\Big)\\
&\quad + \frac{1}{2}\Big((k_1 + k_2)x_{10}^2 + (k_2 + k_3)x_{20}^2 + k_3x_{30}^2\Big).
\end{aligned}$$

The three terms on the right-hand side in (26) with μ are the frictional energy dissipation and are always nonpositive. A steady state is reached at finite time $\hat{t} > 0$, when $v_1 = v_2 = v_3 = 0$, and then the energy balance is that of the elastic potential energy, $E(t) = E_p(t)$, which holds for all $t \geq \hat{t}$.

7. Numerical Schemes

This section constructs numerical schemes for computer simulations of the problems. These are based on the so called 'one-step θ scheme'. In this way, a convex lin-

ear combination is obtained and used in two consecutive time-step solutions. We let $0 = t_0 < t_1 < \cdots < t_N = T$ be a uniform partition, with time step size $h = t_l - t_{l-1} > 0$, of the time interval, and we denote the numerical solution at time step $t = t_l, l \in \{1, \ldots, N\}$, as

$$\boldsymbol{x}^l = \left(x_1^l,\, v_1^l,\, x_2^l,\, v_2^l,\, x_3^l,\, v_3^l\right)^T.$$

At each time step $t = t_l$, we write

$$x_i(t_l) \approx x_i^l, \quad v_i(t_l) \approx v_i^l, \qquad i = 1, 2, 3.$$

For each $h > 0$ and $1/2 \leq \theta \leq 1$, the numerical trajectories, denoted by $\left(x_i^{h;\theta},\, v_i^{h;\theta}\right)$, are constructed as follows: $x_i^{h;\theta}$ is a piecewise linear interpolant such that

$$x_i^{h;\theta}(t_l) = (1-\theta)x_i^l, \quad x_i^{h;\theta}(t_{l+1}) = \theta x_i^{l+1} \text{ on } [t_l,\, t_{l+1}].$$

Furthermore, $v_i^{h;\theta}$ is a piecewise constant interpolant such that

$$v_i^{h;\theta}(t) = \theta v_i^{l+1} \text{for all } t \in (t_l,\, t_{l+1}], \quad v_i^{h;\theta}(t) = (1-\theta)v_i^l \text{ for all } t \in (t_{l-1},\, t_l].$$

The external force f is assumed to be approximated by a piecewise linear interpolant, denoted by f^θ, such that

$$f^\theta(t_l) = (1-\theta)f(t_l), \quad f^\theta(t_{l+1}) = \theta f(t_{l+1}) \text{ on } [t_l,\, t_{l+1}].$$

Now, we construct the following numerical formulation of recurrence in vector form:

Problem 5. *Given the parameters $\theta \in [0,\, 1]$ and $h > 0$, solve*

$$\frac{1}{h}\boldsymbol{M}\left(\boldsymbol{x}^{l+1} - \boldsymbol{x}^l\right) + \boldsymbol{K}\left(\theta\boldsymbol{x}^{l+1} + (1-\theta)\boldsymbol{x}^l\right) + \boldsymbol{F}^{l;l+1} = \boldsymbol{0}, \tag{27}$$

with the initial conditions $x_i(0) = \overline{x}_i,\ v_i(0) = \overline{v}_i$.

Here, $\boldsymbol{M}$ is a diagonal mass matrix with $\boldsymbol{M} = \left[m_{ij}\right] \equiv a_i\delta_{ij}$, and when $i = 2k$ with $1 \leq k \leq 3$, $a_i = m_i$; otherwise, $a_i = 1$. Furthermore,

$$\boldsymbol{K} = \begin{pmatrix} 0 & -1 & 0 & 0 & 0 & 0 \\ k_1 + k_2 & c_1 + c_2 & -k_2 & -c_2 & 0 & 0 \\ 0 & 0 & 0 & -1 & 0 & 0 \\ -k_2 & -c_2 & k_2 + k_3 & c_2 + c_3 & -k_3 & -c_3 \\ 0 & 0 & 0 & 0 & 0 & -1 \\ 0 & 0 & -k_3 & -c_3 & k_3 & c_3 \end{pmatrix},$$

$$\boldsymbol{F}^{l;l+1} = \begin{pmatrix} 0 \\ m_1 g \frac{\mu\left(v_1^l\right)\left(\theta v_1^{l+1} + (1-\theta)v_1^l\right)}{\sqrt{\left(\theta v_1^{l+1} + (1-\theta)v_1^l\right)^2 + \varepsilon^2}} \\ 0 \\ m_2 g \frac{\mu\left(v_2^l\right)\left(\theta v_2^{l+1} + (1-\theta)v_2^l\right)}{\sqrt{\left(\theta v_2^{l+1} + (1-\theta)v_2^l\right)^2 + \varepsilon^2}} \\ 0 \\ m_3 g \frac{\mu\left(v_3^l\right)\left(\theta v_3^{l+1} + (1-\theta)v_3^l\right)}{\sqrt{\left(\theta v_3^{l+1} + (1-\theta)v_3^l\right)^2 + \varepsilon^2}} - \left(f^\theta(t_l) + f^\theta(t_{l+1})\right) \end{pmatrix},$$

where, the rows of $\boldsymbol{F}^{l;l+1}$ are approximations of the subdifferential inclusions.

Once the solution of (27) at time step l has been found, we employ the Newton–Raphson method to find the numerical solutions of (27) at time step $l+1$. For the given previous data $\boldsymbol{x}^l$, we update $\boldsymbol{x}^{l+1}$ from Newton's iteration. We replace $\boldsymbol{x}^{l+1}$ with $\boldsymbol{z} = (z_1, z_2, z_3, z_4, z_5, z_6)^T$ to define a nonlinear mapping $\boldsymbol{Q} : [0, 1] \times \mathbb{R}_+ \times \mathbb{R}^6 \to \mathbb{R}^6$

$$\boldsymbol{Q}(\theta, h, \boldsymbol{z}) = (Q_1, Q_2, Q_3, Q_4, Q_5, Q_6)^T,$$

where

$$\begin{aligned}
Q_1(\theta,h,\boldsymbol{z}) =& z_1 - x_1^l - h\Big(\theta z_2 + (1-\theta)v_1^l\Big),\\
Q_2(\theta,h,\boldsymbol{z}) =& h\theta(k_1+k_2)z_1 + (m_1 + h\theta(c_1+c_2))z_2 - h\theta k_2 z_3 - h\theta c_2 z_4\\
&+ hm_1 g\frac{\mu\Big(v_1^l\Big)\Big(\theta z_2 + (1-\theta)v_1^l\Big)}{\sqrt{\Big(\theta z_2 + (1-\theta)v_1^l\Big)^2 + \varepsilon^2}} + b_2\Big(x_1^l, v_1^l, x_2^l, v_2^l\Big),\\
Q_3(\theta,h,\boldsymbol{z}) =& z_3 - x_2^l - h\Big(\theta z_4 + (1-\theta)v_2^l\Big),\\
Q_4(\theta,h,\boldsymbol{z}) =& -h\theta k_2 z_1 - h\theta c_2 z_2 + h\theta(k_2+k_3)z_3 + (m_2 + h\theta(c_2+c_3))z_4\\
&- h\theta k_3 z_5 - h\theta c_3 z_6 + hm_2 g\frac{\mu\Big(v_2^l\Big)\Big(\theta z_4 + (1-\theta)v_2^l\Big)}{\sqrt{\Big(\theta z_4 + (1-\theta)v_2^l\Big)^2 + \varepsilon^2}}\\
&+ b_4\Big(x_1^l, v_1^l, x_2^l, v_2^l, x_3^l, v_3^l\Big),\\
Q_5(\theta,h,\boldsymbol{z}) =& z_5 - x_3^l - h\Big(\theta z_5 + (1-\theta)v_3^l\Big),\\
Q_6(\theta,h,\boldsymbol{z}) =& -h\theta k_3 z_3 - h\theta c_3 z_4 + h\theta k_3 z_5 + (m_3 + h\theta c_3)z_6\\
&+ hm_3 g\frac{\mu\Big(v_3^l\Big)\Big(\theta z_6 + (1-\theta)v_3^l\Big)}{\sqrt{\Big(\theta z_6 + (1-\theta)v_3^l\Big)^2 + \varepsilon^2}} + b_6\Big(x_2^l, v_2^l, x_3^l, v_3^l\Big).
\end{aligned}$$

Note that b_2, b_4, and b_6 are written in terms of all the previous steps' solutions:

$$\begin{aligned}
b_2\Big(x_1^l, v_1^l, x_2^l, v_2^l\Big) =& h(1-\theta)(k_1+k_2)x_1^l + (h(1-\theta)(c_1+c_2) - m_1)v_1^l\\
&- h(1-\theta)k_2 x_2^l - h(1-\theta)c_2 v_2^l,\\
b_4\Big(x_1^l, v_1^l, x_2^l, v_2^l, x_3^l, v_3^l\Big) =& -h(1-\theta)k_2 x_1^l - h(1-\theta)c_2 v_1^l + h(1-\theta)(k_2+k_3)x_2^l\\
&+ (h(1-\theta)(c_2+c_3) - m_2)v_2^l - h(1-\theta)k_3 x_3^l\\
&- h(1-\theta)c_3 v_3^l,\\
b_6\Big(x_2^l, v_2^l, x_3^l, v_3^l\Big) =& -h(1-\theta)k_3 x_2^l - h(1-\theta)c_3 v_2^l + h(1-\theta)k_3 x_3^l\\
&+ (h(1-\theta)c_3 - m_3)v_3^l - h\Big(f^\theta(t_l) + f^\theta(t_{l+1})\Big).
\end{aligned}$$

Now, we can obtain the Jacobian matrix $\nabla_{\boldsymbol{z}}\boldsymbol{Q} : [0, 1] \times \mathbb{R}_+ \times \mathbb{R}^6 \to \mathbb{R}^{6\times 6}$:

$$\nabla_{\boldsymbol{z}}\boldsymbol{Q}(\theta,h,\boldsymbol{z}) = \begin{bmatrix}
1 & -h\theta & 0 & 0 & 0 & 0\\
h\theta(k_1+k_2) & j_{22} & -h\theta k_2 & -h\theta c_2 & 0 & 0\\
0 & 0 & 1 & -h\theta & 0 & 0\\
-h\theta k_2 & h\theta c_2 & h\theta(k_2+k_3) & j_{44} & -h\theta k_3 & -h\theta c_3\\
0 & 0 & 0 & 0 & 1 & -h\theta\\
0 & 0 & -h\theta k_3 & -h\theta c_3 & h\theta k_3 & j_{66}
\end{bmatrix},$$

where

$$j_{22} = m_1 + h\theta\left((c_1 + c_2) + \frac{m_1 g\mu\left(v_1^l\right)\varepsilon^2}{\left(\left(\theta z_2 + (1-\theta)v_1^l\right)^2 + \varepsilon^2\right)^{3/2}}\right),$$

$$j_{44} = m_2 + h\theta\left((c_2 + c_3) + \frac{m_2 g\mu\left(v_2^l\right)\varepsilon^2}{\left(\left(\theta z_4 + (1-\theta)v_2^l\right)^2 + \varepsilon^2\right)^{3/2}}\right),$$

$$j_{66} = m_3 + h\theta\left(c_3 + \frac{m_3 g\mu\left(v_2^l\right)\varepsilon^2}{\left(\left(\theta z_4 + (1-\theta)v_2^l\right)^2 + \varepsilon^2\right)^{3/2}}\right),$$

The determinant of the Jacobian matrix is as follows:

$$\begin{aligned}
&|\nabla_z Q(z)| \\
&= j_{22}\left(j_{44}\left(j_{66} + h^2\theta^2 k_3\right) + h^2\theta^2 j_{66}\left(-c_3^2 + j_{66}(k_2 + k_3) - 2h\theta k_3 c_3 + h^2\theta^2 k_2 k_3\right)\right) \\
&+ h^2\theta^2\left(c_2^2\left(j_{66} + h^2\theta^2 k_3 + j_{44}(k_1 + k_2)\right)\left(j_{66} + h^2\theta^2 k_3\right)\right. \\
&\left.+ h^2\theta^2\left(-c_3^2(k_1 + k_2) + j_{66}k_2k_3 + j_{66}k_1(k_2 + k_3) - 2h\theta c_3(k_1 + k_3) + h^2\theta^2 k_1 k_2 k_3\right)\right) \\
&= j_{22}\left(j_{44}\left(j_{66} + O\left(h^2\right) + O\left(h^2\right)\left(-c_3^2 + j_{66}(k_2 + k_3) - O(h) + O\left(h^2\right)\right)\right)\right) \\
&+ O\left(h^2\right)\left(c_2^2 j_{66} + O\left(h^2\right) + j_{44}(k_1 + k_2)\right)\left(j_{66} + O\left(h^2\right)\right) \\
&+ O\left(h^2\right)\left(-c_3^2(k_1 + k_2) + j_{66}k_2k_3 + j_{66}k_1(k_2 + k_3) - O(h) + O\left(h^2\right)\right),
\end{aligned}$$

where big O notation is used. Since $h > 0$ can be chosen to be sufficiently small, we can obtain

$$\begin{aligned}
&|\nabla_z Q(z)| \approx j_{22}j_{44}j_{66} \\
&= (m_1 + O(h))(m_2 + O(h))(m_3 + O(h)) \approx m_1 m_2 m_3 > 0,
\end{aligned}$$

which shows that it is a positive definite matrix. We write the formula for Newton's iteration with a fixed $h > 0$ as

$$z_{k+1} = z_k - [\nabla_z \boldsymbol{Q}(h, z_k)]^{-1}\boldsymbol{Q}(h, z_k) \text{ for } \quad k \geq 0, \tag{28}$$

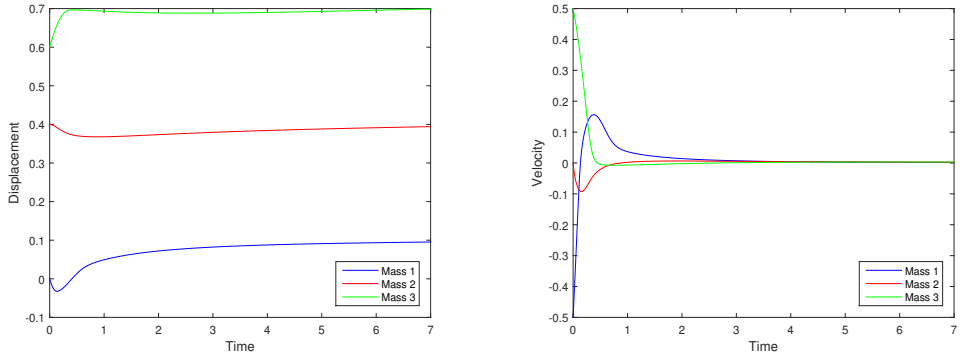
where $\{z_k \mid k \geq 1\}$ is a sequence of iterates to find the next step's numerical solution $\boldsymbol{x}^{l+1}$. In the iteration process, the initial guess z_0 is assigned by the previous time step's solution $\boldsymbol{x}^l$. Gaussian elimination is used during each iteration to solve the system in (28).

8. Numerical Experiments

We use the numerical schemes above to perform numerical experiments, or simulations, starting with typical behavior as the baseline simulation. Then, we show the appearance of a detachment wave. A more theoretical part is provided in the next section, where we compare the schemes with different θ values.

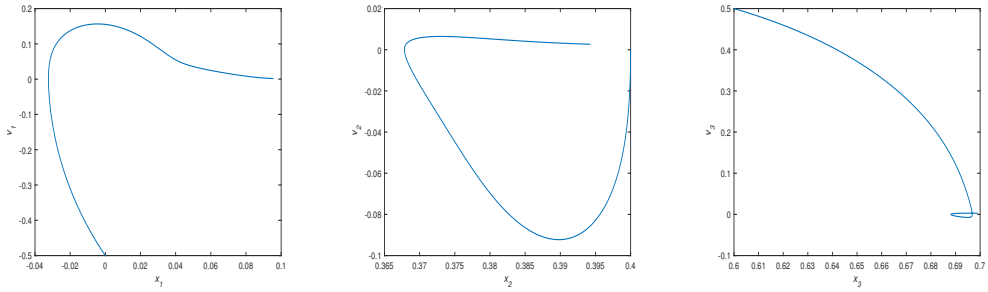
In all simulations, the friction function is $\mu(v) = 0.2\exp\left(-0.1v^2\right)$, the time step size is $h = 2 \times 10^{-4}$, and the smoothing parameter is $\varepsilon = 1/10$. In particular, $\theta = 1/2$ is chosen in the numerical simulations, shown in Figures 3–7. The data used in the baseline simulation are presented in Table 1. In the numerical computations, when we update the next time step's numerical approximation $\boldsymbol{x}^{l+1}$ from the linear system in (28), we utilize MATLAB's sparse matrix data structure to save memory. The elapsed computation time for all the

simulations is, on average, about 30 s. Thus, it takes about 8×10^{-4} s to compute each time step's approximation. In addition, the average number of Newton's iterations per time step is about six. We note that the number of iterations decreases if the smoothing parameters $\varepsilon > 0$ are greater than $\varepsilon = 1/10$. Over all the numerical experiments, we did not observe any computational delays.



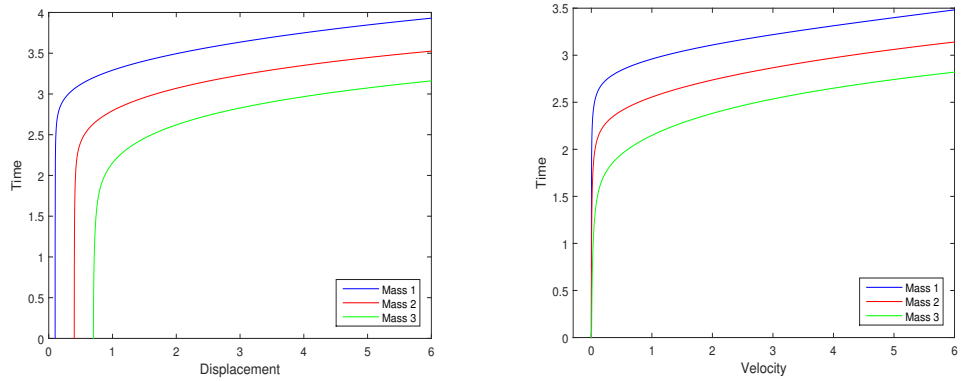
(**a**) Displacements (**b**) Velocities

Figure 3. Baseline simulation. The motion of the three masses for $f = 0.5$; the system starts moving at $t = 0$ and approaches the steady state at $t > 4$.



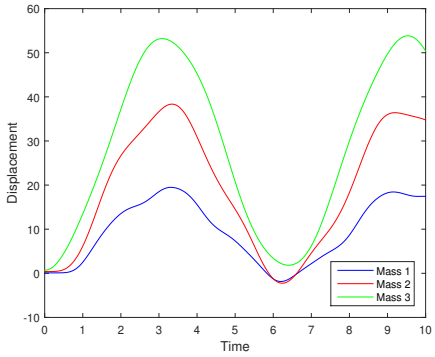
(**a**) (x_1, v_1) (**b**) (x_2, v_2) (**c**) (x_3, v_3)

Figure 4. Baseline simulation showing system trajectories in the phase planes (x_i, v_i).

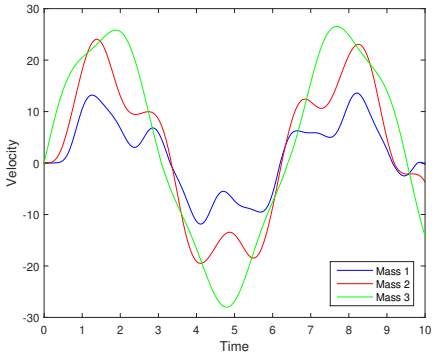


(**a**) Displacement (**b**) Velocity

Figure 5. Slip initiation: mass m_3 moves first, then m_2, and finally m_1 starts sliding. Note that the vertical axis is the time axis.

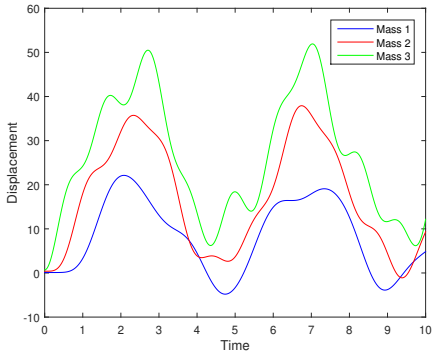


(**a**) Displacements

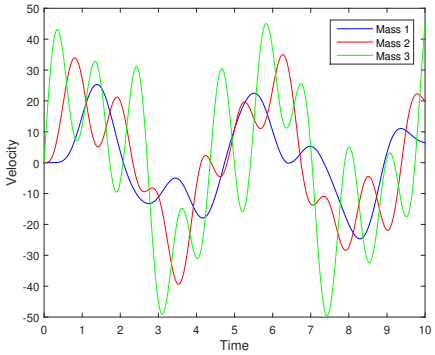


(**b**) Velocities

Figure 6. $m_1 = 2$, $m_2 = 6$, $m_3 = 12$.



(**a**) Displacements



(**b**) Velocities

Figure 7. $m_1 = 12$, $m_2 = 6$, $m_3 = 2$.

Table 1. The baseline data.

m_1	m_2	m_3	k_1	k_2	k_3	c_1	c_2	c_3	T
5 kg	5 kg	5 kg	45 N/m	45 N/m	45 N/m	0 kg /s	0 kg /s	0 kg /s	7 s

For simplicity, we omit the SI base units used in Table 1. All springs are assumed to be purely elastic, and the masses are equal. Additionally, their equilibrium positions are assumed to be $\hat{x}_1 = 0.1$, $\hat{x}_2 = 0.4$, and $\hat{x}_3 = 0.7$. The initial conditions in the baseline are as follows:

$$\overline{x}_1 = -0.1, \quad \overline{x}_2 = 0, \quad \overline{x}_3 = 0.1, \quad \overline{v}_1 = -0.5, \quad \overline{v}_2 = 0, \quad \overline{v}_3 = 0.5.$$

The results of the baseline simulations are shown in Figures 3 and 4. Figure 3 shows the evolution of the displacements of the masses (a) and of the velocities (b). In this case, the system starts moving at $t = 0$, since the applied force is sufficient to overcome the static friction resistance. The approach to steady state is clearly visible for $t > 4$. Figure 4 shows the trajectories in the phase planes (x_1, v_1), (x_2, v_2), and (x_3, v_3). The energy dissipation of the system is clearly seen, as it approaches its steady state in finite time.

The next simulation, Figure 5, shows the beginning of a slip motion. It uses an increasing external force $f(t) = 0.5e^{2t}$ and the following initial data:

$$\overline{x}_1 = \overline{x}_2 = \overline{x}_3 = 0, \quad \overline{v}_1 = \overline{v}_2 = \overline{v}_3 = 0.$$

It can be seen that mass m_3 starts slipping at time t_{l_3} when $f(t_{l_3}) > f^* = \mu m_3 g$. After that, mass m_2 starts moving at time t_{l_2} when $f(t_{l_2}) > f^* = \mu(m_2 + m_3)g + k_3(L_3^+ - L_2^+)$. Finally, mass m_1 starts moving at time t_{l_1} when $f(t_{l_1}) > f^* = \mu(m_1 + m_2 + m_3)g + k_3(L_3^+ - L_2^+) + k_2(L_2^+ - L_1^+)$. Since the force is monotonically increasing, once the masses start moving, the displacements are monotonically increasing. Additional information is given in Table 2, where we provide the times when the slip starts, the force at that time, and the critical force.

Table 2. Slip initiation details: the time of initiation t_{l_i}; the value of the force $f(t_{l_i})$, $i = 1, 2, 3$; and the critical value f^*.

	m_3	m_2	m_1
t_{l_i}	1.4880	2.7242	3.2286
$f(t_{l_i})$	9.8027	116.1698	318.5734
f^*	9.8000	116.1400	318.5200

For the sake of completeness, we performed two simulations with unequal masses. The third simulation used unequal masses in two configurations with a large constant force $f = 400$ and $T = 10$. The simulation results are depicted in Figure 6. It can be seen that the oscillations are not periodic, with mass m_3 oscillating the least, while mass m_1 the most. The velocities seem to be somewhat reflected at $t \approx 5$. Next, in the opposite configuration, Figure 7, it is seen that the oscillations are not periodic, either, with mass m_3 oscillating the most and mass m_1 the least. It may be of interest to investigate such cases further and possibly establish that the motion is chaotic.

9. Numerical Assessments

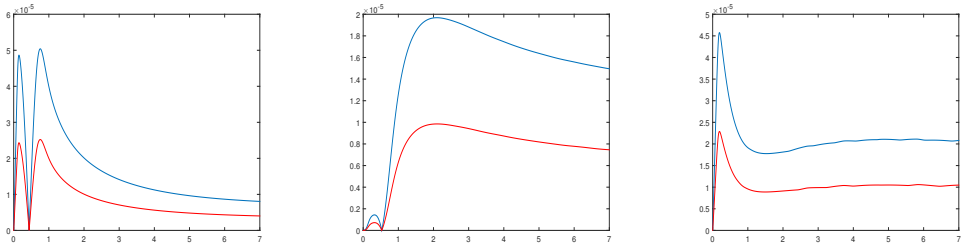
This section provides insights into a few aspects of the numerical schemes used in this work. The numerical assessment is based on Table 1.

9.1. Numerical Assessment of the Algorithm

First, we assess the accuracy of the simulations. We recall that the values $\theta = 0, 1/2, 1$ correspond to numerical formulations of the 'explicit Euler method', the 'Crank–Nicholson method', and the 'implicit Euler method', respectively. Note that the average number of Newton's iterations for all three choices of θ is found to be around seven. According to the numerical estimates, the differences become smaller as $h \downarrow 0$. We turn to the differences in the solutions with $\theta = 1/2$, $\theta = 3/4$, and $\theta = 1$. These are given as follows:

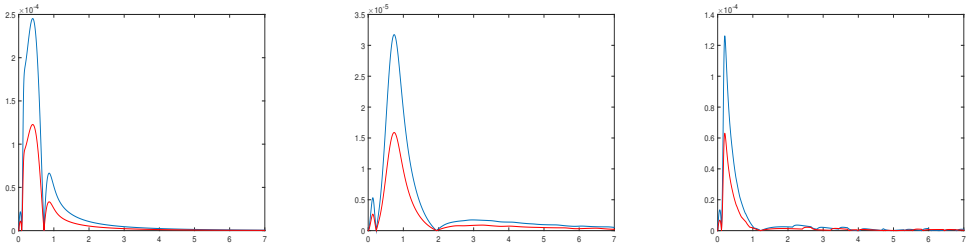
$$\max_{1\le i\le 3}\max_{0\le t\le 7}\left|x_i^{h;\theta=1/2}(t) - x_i^{h;\theta=3/4}(t)\right| \approx 2.5224 \times 10^{-5},$$
$$\max_{1\le i\le 3}\max_{0\le t\le 7}\left|x_i^{h;\theta=1/2}(t) - x_i^{h;\theta=1}(t)\right| \approx 5.0402 \times 10^{-5},$$
$$\max_{1\le i\le 3}\max_{0\le t\le 7}\left|v_i^{h;\theta=1/2}(t) - v_i^{h;\theta=3/4}(t)\right| \approx 1.2270 \times 10^{-4},$$
$$\max_{1\le i\le 3}\max_{0\le t\le 7}\left|v_i^{h;\theta=1/2}(t) - v_i^{h;\theta=1}(t)\right| \approx 2.4258 \times 10^{-4}.$$

In Figures 8 and 9, the blue curves show the differences between the approximations with $\theta = 1/2$ and $\theta = 1$. We assume that $x_i^{h;\theta=1/2}$, $x_i^{h;\theta=1}$, and $x_i^{h;\theta=3/4}$ denote the corresponding numerical trajectories for the exact solutions x_i. Similarly, the red curves in each picture show the differences between the approximations with $\theta = 1/2$ and $\theta = 3/4$.



(**a**) For x_1 (**b**) For x_2 (**c**) For x_3

Figure 8. Differences or errors in displacement.



(**a**) For v_1 (**b**) For v_2 (**c**) For v_3

Figure 9. Gaps for velocity.

9.2. Numerical Reachability

Now, we provide brief numerical evidence for the conjecture concerning *reachability*. Based on the data in Table 1, the stick regions are as follows:

$$\begin{aligned} L_1^- &= -6.3916, \quad L_1^+ = 6.4138, \quad L_2^- = -10.6489, \\ L_2^+ &= 10.6933, \quad L_3^- = -12.7720, \quad L_3^+ = 12.8387. \end{aligned} \tag{29}$$

As we can observe in (a) and (b) in Figure 3, the steady state is attained around $t = 5.5$. It can be seen that all the masses reach $0.1 \leq \tilde{x}_i \leq 0.7$, satisfying the stick states shown in (29). The chosen initial data support the argument that $(x_i(t), v_i(t)) \to (\tilde{x}_i, 0)$ as $t \to \infty$. We note that if the magnitude of $f > 0$ were large, a much larger time limit for simulations would be required. From a physical point of view, the masses can attain the steady states sooner if the masses are heavier or the springs are stiffer, which has also been found in our other numerical experiments.

9.3. Numerical Support for the Energy Balance

As was discussed in Section 6, concerning the energy balance in the steady state, numerical evidence that our scheme preserve the energy balance is presented in Figure 10b. We observe that the curves meet around $t = 4$. Note that the blue and red color curves show E^l and E_p^l, respectively. Moreover, the red curve in Figure 10a shows the energy dissipation caused by friction.

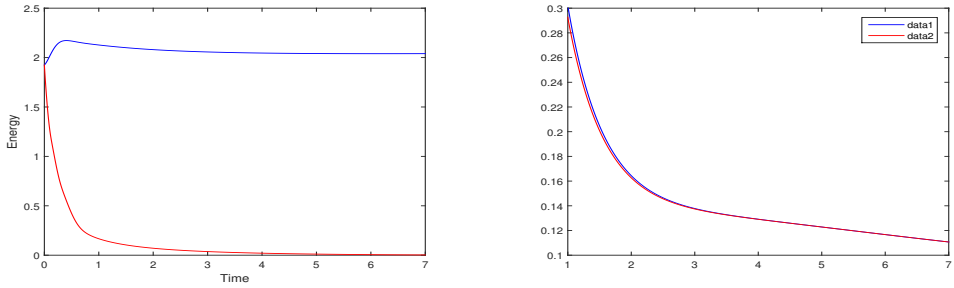
We next show that our scheme preserves energy. In the discrete case, the total energy function at each time step $t = t_l$ for the system is defined by

$$E_D(t_l) := E^l = E_k^l + E_p^l,$$

where

$$E_k^l = \frac{1}{2}m_1\left(v_1^l\right)^2 + \frac{1}{2}m_2\left(v_2^l\right)^2 + \frac{1}{2}m_3\left(v_3^l\right)^2,$$
$$E_p^l = \frac{1}{2}\left((k_1+k_2)\left(x_1^l\right)^2 + (k_2+k_3)\left(x_2^l\right)^2 + k_3\left(x_3^l\right)^2\right).$$

The numerical energy balance is justified in the following Proposition 2.



(**a**) Frictional energy loss (**b**) In the steady state

Figure 10. Energy balance.

Proposition 2. *Assume that* $\boldsymbol{x}^l$ *satisfies the numerical formulation (27) at time step* $t = t_l$ *and the initial data* $x_i(0) = \bar{x}_i \in \mathbb{R}$ *and* $v_i(0) = \bar{v}_i \in \mathbb{R}$. *If* $\theta \in [1/2, 1]$ *and* $c_1 = c_2 = c_3 = 0$, *then*

$$E^0 + k_2\left(\int_0^{t_l} x_2^{h;\theta}(t)v_1^{h;\theta}(t) + x_1^{h;\theta}(t)v_2^{h;\theta}(t)\,dt\right) + \int_0^{t_l} f^\theta(t)v_3^{h;\theta}(t)dt$$
$$+ k_3\left(\int_0^{t_l} x_3^{h;\theta}(t)v_2^{h;\theta}(t) + x_2^{h;\theta}(t)v_3^{h;\theta}(t)\,dt\right) \geq E^l \text{ for any } l \geq 1. \tag{30}$$

Proof. We use (27) to write the following three equations:

$$\frac{m_1}{h}\underbrace{\left(v_1^{l+1}-v_1^l\right)\left(\theta v_1^{l+1}+(1-\theta)v_1^l\right)}_{I_1^v} + \frac{(k_1+k_2)}{h}\underbrace{\left(\theta x_1^{l+1}+(1-\theta)x_1^l\right)\left(x_1^{l+1}-x_1^l\right)}_{I_1^x}$$
$$+ m_1 g\frac{\mu\left(v_1^l\right)\left(\theta v_1^{l+1}+(1-\theta)v_1^l\right)^2}{\sqrt{\left(\theta v_1^{l+1}+(1-\theta)v_1^l\right)^2+\varepsilon^2}} = k_2\underbrace{\left(\theta x_2^{l+1}+(1-\theta)x_2^l\right)\left(\theta v_1^{l+1}+(1-\theta)v_1^l\right)}_{II},$$

$$\frac{m_2}{h}\underbrace{\left(v_2^{l+1}-v_2^l\right)\left(\theta v_2^{l+1}+(1-\theta)v_2^l\right)}_{I_2^v} + \frac{(k_2+k_3)}{h}\underbrace{\left(\theta x_2^{l+1}+(1-\theta)x_2^l\right)\left(x_2^{l+1}-x_2^l\right)}_{I_2^x}$$
$$+ m_2 g\frac{\mu\left(v_2^l\right)\left(\theta v_2^{l+1}+(1-\theta)v_2^l\right)^2}{\sqrt{\left(\theta v_2^{l+1}+(1-\theta)v_2^l\right)^2+\varepsilon^2}} = k_2\underbrace{\left(\theta x_1^{l+1}+(1-\theta)x_1^l\right)\left(\theta v_2^{l+1}+(1-\theta)v_2^l\right)}_{III}$$
$$+ k_3\underbrace{\left(\theta x_3^{l+1}+(1-\theta)x_3^l\right)\left(\theta v_2^{l+1}+(1-\theta)v_2^l\right)}_{IV},$$

and

$$\frac{m_3}{h}\underbrace{\left(v_3^{l+1}-v_3^l\right)\left(\theta v_3^{l+1}+(1-\theta)v_3^l\right)}_{I_3^v}+\frac{k_3}{h}\underbrace{\left(\theta x_3^{l+1}+(1-\theta)x_3^l\right)\left(x_3^{l+1}-x_3^l\right)}_{I_3^x}$$
$$+m_2g\frac{\mu\left(v_3^l\right)\left(\theta v_3^{l+1}+(1-\theta)v_3^l\right)^2}{\sqrt{\left(\theta v_3^{l+1}+(1-\theta)v_3^l\right)^2+\varepsilon^2}}=k_3\underbrace{\left(\theta x_2^{l+1}+(1-\theta)x_2^l\right)\left(\theta v_3^{l+1}+(1-\theta)v_3^l\right)}_{V}$$
$$+\underbrace{(\theta f(t_{l+1})+(1-\theta)f(t_l))\left(\theta v_3^{l+1}+(1-\theta)v_3^l\right)}_{VI}.$$

It follows from I_i^v with $1\le i\le 3$ that

$$\begin{aligned}I_v^i&=\left(v_i^{l+1}-v_i^l\right)\left(\theta v_i^{l+1}+(1-\theta)v_i^l\right)\\&=\theta\left(v_i^{l+1}\right)^2-\theta\left(v_i^l\right)^2-(1-2\theta)\left(v_i^l\right)^2+(1-2\theta)v_i^{l+1}v_i^l\\&=\theta\left(v_i^{l+1}\right)^2-\theta\left(v_i^l\right)^2-\frac{(1-2\theta)}{2}\left(v_i^l-v_i^{l+1}+v_i^l+v_i^{l+1}\right)^2\left(v_i^l-v_i^{l+1}\right)\\&=\theta\left(v_i^{l+1}\right)^2-\theta\left(v_i^l\right)^2-\frac{(1-2\theta)}{2}\left(\left(v_i^l-v_i^{l+1}\right)^2+\left(v_i^l\right)^2-\left(v_i^{l+1}\right)^2\right).\end{aligned}\tag{31}$$

Since $\theta\in[1/2,\,1]$, we can see from (31) that

$$I_i^v\ge\frac{1}{2}\left(\left(v_i^{l+1}\right)^2-\left(v_i^l\right)^2\right).\tag{32}$$

By a similar argument, we find

$$I_i^x\ge\frac{1}{2}\left(\left(x_i^{l+1}\right)^2-\left(x_i^l\right)^2\right).\tag{33}$$

Using (32) and (33), we arrive at the following estimate:

$$\begin{aligned}&E^l+h(k_2(II+III)+k_3(IV+V)+VI)\\&\quad\ge E^{l+1}+h\sum_{i=1}^{3}m_ig\frac{\mu\left(v_i^l\right)\left(\theta v_i^{l+1}+(1-\theta)v_i^l\right)^2}{\sqrt{\left(\theta v_i^{l+1}+(1-\theta)v_i^l\right)^2+\varepsilon^2}}.\end{aligned}\tag{34}$$

Since for each $1\le i\le 3$,

$$m_ig\frac{\mu\left(v_i^l\right)\left(\theta v_i^{l+1}+(1-\theta)v_i^l\right)^2}{\sqrt{\left(\theta v_i^{l+1}+(1-\theta)v_i^l\right)^2+\varepsilon^2}}\ge 0,$$

it follows from (34) that

$$E^l+h(k_2(II+III)+k_3(IV+V)+VI)\ge E^{l+1}.$$

Now, recalling the construction of numerical trajectories, we obtain

$$\begin{aligned}&\int_{t_l}^{t_{l+1}} x_i^{h;\theta}(t)v_j^{h;\theta}(t)dt\\&\quad= h\Big(\theta x_i^{l+1}+(1-\theta)x_i^l\Big)\Big(\theta v_j^{l+1}+(1-\theta)v_j^l\Big)\end{aligned}$$

for $1 \leq i, j \leq 3$, and

$$\begin{aligned}&\int_{t_l}^{t_{l+1}} f^\theta(t)v_3^{h;\theta}(t)dt\\&\quad= h(\theta f(t_{l+1})+(1-\theta)f(t_l))\Big(\theta v_3^{l+1}+(1-\theta)v_3^l\Big).\end{aligned}$$

The telescoping series allows us to have the estimate (30), as desired. □

We use the trapezoidal rule to assume that, for each $1 \leq i \leq 3$,

$$\frac{h}{2}\frac{\mu\Big(v_i^l\Big)\Big(\theta v_i^{l+1}+(1-\theta)v_i^l\Big)^2}{\sqrt{\Big(\theta v_i^{l+1}+(1-\theta)v_i^l\Big)^2+\varepsilon^2}}=\int_{t_l}^{t_{l+1}}\frac{\mu\Big(v_i^{h;\theta}(t)\Big)\Big(v_i^{h;\theta}(t)\Big)^2}{\sqrt{\Big(v_i^{h;\theta}(t)\Big)^2+\varepsilon^2}}dt.$$

We can observe from the previous Proposition (Proposition 2) that if $\theta = 1/2$, we can have an energy balance form in the discrete case

$$\begin{aligned}&E^0+k_2\int_0^{t_l}x_2^{h;\theta}(t)v_1^{h;\theta}(t)+x_1^{h;\theta}(t)v_2^{h;\theta}(t)\,dt+\int_0^{t_l}f^\theta(t)v_3^{h;\theta}(t)dt\\&\quad+k_3\int_0^{t_l}x_3^{h;\theta}(t)v_2^{h;\theta}(t)+x_2^{h;\theta}(t)v_3^{h;\theta}(t)\,dt=E^l\\&\quad+2\sum_{i=1}^{3}m_ig\int_0^{t_l}\frac{\mu\Big(v^{h;\theta}(t)\Big)\Big(v^{h;\theta}(t)\Big)^2}{\sqrt{\Big(v^{h;\theta}(t)\Big)^2+\varepsilon^2}}dt.\end{aligned}\tag{35}$$

It is worth noticing that the last term in (35) is a numerical approximation of the frictional energy loss. As we can see in Figure 10a, the gap between the blue line and the red line shows the energy loss. In addition, the uniform difference of both sides in (35) is computed as follows:

$$\begin{aligned}&\max_{0\leq t\leq T}\Bigg|E^0+k_2\int_0^t x_2^{h;\theta}(\tau)v_1^{h;\theta}(\tau)+x_1^{h;\theta}(\tau)v_2^{h;\theta}(\tau)\,d\tau+\int_0^t f^\theta(\tau)v_3^{h;\theta}(\tau)d\tau\Big)\\&\quad+k_3\int_0^t x_3^{h;\theta}(\tau)v_2^{h;\theta}(\tau)+x_2^{h;\theta}(\tau)v_3^{h;\theta}(\tau)\,d\tau-E_D(t)\\&\quad-2\sum_{i=1}^{3}m_ig\int_0^t\frac{\mu\Big(v^{h;\theta}(\tau)\Big)\Big(v^{h;\theta}(\tau)\Big)^2}{\sqrt{\Big(v^{h;\theta}(\tau)\Big)^2+\varepsilon^2}}d\tau\Bigg|=0.0756.\end{aligned}\tag{36}$$

We can also observe that $\theta = 3/4$ and $\theta = 1$ give uniform differences of 0.0016 and 0.0066, respectively.

10. Conclusions and Future Work

This work studies, analyzes, and simulates a mathematical model for the motion, under an applied force, of a system of three masses connected with springs and dampers when frictional resistance is included. Adding friction changes the system into a differential set-valued inclusion. It is found that even such a 'simple' problem poses considerable

mathematical challenges. Indeed, in the dynamic case, we use the general existence and uniqueness theorem, Theorem 5.1 in [3], to deduce the existence and uniqueness of the system's weak solution. On the other hand, the quasistatic case makes it necessary to use a more elaborate result, establishing the existence of weak solutions; however, their uniqueness is still open.

The original motivation for this work, following [1], was to mathematically and numerically study the initiation of slip motion in systems with friction, i.e., the generation of detachment waves. The mathematical complexity of the problem is found to be rather an interesting surprise.

We provide a comprehensive study of the steady states of the system, which are the *stick states* in which the masses are static because of sufficient frictional resistance. We conjecture that each steady state may be the long-time limit of a dynamical process with appropriately chosen initial data. The computer simulations support the theory and the conjecture and provide insight into the system's behavior, especially the initiation of detachment waves.

Some issues have not been resolved yet; further studies should be conducted for the following purposes:

- To determine whether the quasistatic problem may actually have multiple solutions or whether the lack of uniqueness is a mathematical artifact;
- To extend the model to include randomness in friction, which is a characteristic of surfaces in contact;
- To extend the analysis of slip initiation;
- To extend the model, analysis, and simulations to a system of n masses and correlate the waves to the system parameters;
- To pass to the continuous limit, $n \to \infty$, and study detachment waves in rods;
- To study detachment waves in beams;
- To study detachment waves in more complex systems and correlate the waves with the system parameters.

Since the long-term interest is centered around the detachment waves, one of the next stages of this research will include adding the dynamics of the surface asperities that are involved in friction, particularly their elastic or plastic deformations and possible breakage, causing debris on the surface.

Author Contributions: Both authors contributed to the writing, model and analysis equally, while J.A. also performed the numerical analysis and conducted the simulations. All authors have read and agreed to the published version of the manuscript.

Funding: This research received no external funding.

Data Availability Statement: Data are contained within the article.

Acknowledgments: The authors would like to acknowledge the helpful and thorough comments of the anonymous referees, which have improved the presentation of this paper. The second author (M.S.) is grateful for the travel support received from the grant Nonsmooth Contact Dynamics CONMECH, supported by the European Union's Framework Programme for Research and Innovation Horizon 2024.

Conflicts of Interest: The authors declare no conflicts of interest.

References

1. Shillor, M.; Kuttler, K.L. Detachment waves in frictional contact: I—A two-mass system. *Nonlinear Anal. RWA* **2023**, *73*, 103907. [CrossRef]
2. Shillor, M.; Ahn, J. Detachment waves in frictional contact: Analysis and simulations of two-mass system. In *Nonsmooth Problems with Applications in Mechanics*; Migorski, S., Sofones, M., Eds.; Banach Center Publications: Warsaw, Poland, 2024; Volume 127.
3. Kuttler, K.L.; Shillor, M. Set-valued pseudomonotone maps and degenerate evolution inclusions. *Commun. Contemp. Math.* **1999**, *1*, 87–123. [CrossRef]
4. Cochard, A.; Rice, J.R. Fault rupture between dissimilar materials: Ill-posedness, regularization, and slip-pulse response. *J. Geophys. Res. B* **2000**, *105*, 25891–25907. [CrossRef]
5. Scholz, C.H. Earthquakes and friction laws. *Nature* **1998**, *391*, 37–42. [CrossRef]
6. Rubinstein, S.M.; Cohen, G.; Fineberg, J. Detachment fronts and the onset of dynamic friction. *Nature* **2004**, *430*, 1005–1009. [CrossRef] [PubMed]
7. Rubinstein, S.M.; Cohen, G.; Fineberg, J. Dynamics of Precursors to Frictional Sliding. *Phys. Rev. Lett.* **2007**, *98*, 226103. [CrossRef] [PubMed]
8. Borri-Brunetto, M.; Chiaia, B.; Ciavarella, M. Incipient sliding of rough surfaces in contact: A multiscale numerical analysis. *Comput. Methods Appl. Mech. Eng.* **2001**, *190*, 6053–6073. [CrossRef]
9. Ciavarella, M. The generalized Cattaneo partial slip plane contact problem. I-Theory, II-Examples. *Int. J. Solids Struct.* **1998**, *35*, 2349–2378. [CrossRef]
10. Bangerth, W.; Geiger, M.; Rannacher, R. Adaptive Galerkin finite element methods for the wave equation. *Comput. Methods Appl. Math.* **2010**, *10*, 2–48. [CrossRef]
11. Kikuchi, N.; Oden, J.T. *Contact Problems in Elasticity: A Study of Variational Inequalities and Finite Element Methods*; SIAM: Philadelphia, PA, USA, 1988.
12. Sofonea, M.; Matei, A. *Mathematical Models in Contact Mechanics*; Cambridge University Press: Cambridge, UK, 2012.
13. Sofonea, M.; Migorski, S. *Variational-Hemivariational Inequalities with Applications*; Chapman and Hall/CRC: Boca Raton, FL, USA, 2017. [CrossRef]
14. Han, W.; Sofonea, M. *Quasistatic Contact Problems in Viscoelasticity and Viscoplasticity*; AMS/IP: Providence, IR, USA, 2002.
15. Han, W.; Sofonea, M. Numerical analysis of hemivariational inequalities in contact mechanics. *Acta Numer.* **2019**, *28*, 175–286. [CrossRef]
16. Zavarise, G.; Wriggers, P. (Eds.) *Trends in Computational Contact Mechanics*; Springer: Berlin/Heidelberg, Germany, 2011.
17. Kuttler, K.L. Nondegenerate implicit evolution inclusions. *Electron. Differ. Eq.* **2000**, *2000*, 1–20.

Disclaimer/Publisher's Note: The statements, opinions and data contained in all publications are solely those of the individual author(s) and contributor(s) and not of MDPI and/or the editor(s). MDPI and/or the editor(s) disclaim responsibility for any injury to people or property resulting from any ideas, methods, instructions or products referred to in the content.